Neutrino-Mass-Driven Instabilities as the Earliest Flavor Conversion in Supernovae

Damiano F. G. Fiorillo[1,*] Hans-Thomas Janka[2] and Georg G. Raffelt[3]

[1]*Deutsches Elektronen-Synchrotron DESY, Platanenallee 6, 15738 Zeuthen, Germany*
[2]*Max-Planck-Institut für Astrophysik, Karl-Schwarzschild-Strasse 1, 85748 Garching, Germany*
[3]*Max-Planck-Institut für Physik, Boltzmannstrasse 8, 85748 Garching, Germany*

Collective neutrino flavor conversions in core-collapse supernovae begin with instabilities, initially triggered when the dominant ν_e outflow concurs with a small antineutrino flux of opposite lepton number, with $\bar{\nu}_e$ dominating over $\bar{\nu}_\mu$. When these "flipped" neutrinos emerge in the energy-integrated angular distribution (angular crossing), they initiate a fast instability. However, before such conditions arise, spectral crossings typically appear within 20 ms of collapse, i.e., local spectral excesses of $\bar{\nu}_e$ over $\bar{\nu}_\mu$ along some direction. Therefore, postprocessing supernova simulations cannot consistently capture later fast instabilities because the early slow ones have already altered the conditions.

Introduction—At the end of its life, the core of a massive star collapses and forms a protoneutron star (PNS). It releases an intense flux of neutrinos, which likely is the primary driver of the subsequent supernova (SN) explosion [1–3]. Neutrinos depositing energy in the gain region revive the stalled shock wave, thereby triggering the delayed explosion. They also regulate nucleosynthesis in the ejecta. Neutrino interactions, which strongly depend on flavor, are thus key microphysical ingredients in these spectacular cosmic fireworks.

Intriguingly, when neutrinos are dense, their flavor evolution famously remains an open challenge [4–6]. Collective flavor conversions (CFCs) dominate—flavor exchange among neutrinos driven by the coherent weak field they themselves generate. This process is akin to energy exchange between electrons via electric fields in a plasma. Though typically negligible, this weak field can grow exponentially, representing a flavor instability, which occurs when the dominant ν_e outflow is accompanied by a small excess in the energy and angular distribution of opposite lepton number (flipped neutrinos [7]). Such instabilities may develop below the shock wave and could alter energy deposition and the explosion dynamics [8–11].

Instability is a diagnostic tool: SN simulations neglect flavor conversions, so instabilities reveal inconsistency of the subsequent evolution. Johns has stressed the corresponding inconsistency in mapping a preinstability to postinstability configuration [12]. When an instability arises, it disrupts the evolution rendering later ones unphysical. The only meaningful concept is that of weak instabilities that emerge gradually from a previously stable configuration [7,13]. Most attention has focused on fast instabilities [14], which grow within tens of picoseconds and thus appear particularly disruptive. However, not the fastest instabilities are most significant, but rather the first ones to appear, as these will shape the subsequent evolution. This is the key message of this Letter.

Fast instabilities require angular crossings (the distribution flipping from ν_e to $\bar{\nu}_e$ dominance), which may or may not occur in 1D simulations [15–19], while they seem generic after some 100 ms in multidimensional models [20–26]. In contrast, "slow" instabilities, those induced by neutrino masses, require only a spectral crossing: dominance in some energy interval of $\bar{\nu}_e$ over $\bar{\nu}_\mu$ ($\bar{\nu}$ crossing) or of ν_μ over ν_e (ν crossing). Such CFCs consist of pairwise, collisionless conversions $\bar{\nu}_e\nu_e \rightarrow \bar{\nu}_\mu\nu_\mu$ or $\nu_e\nu_\mu \rightarrow \nu_\mu\nu_e$, reshuffling lepton number across the energy distribution. They are triggered by a sign change of the difference of ν_e and ν_μ lepton number (DLN), defined as $n_{\rm DLN} = n_{\nu_e} - n_{\nu_\mu}$ for neutrinos and $n_{\rm DLN} = n_{\bar{\nu}_\mu} - n_{\bar{\nu}_e}$ for antineutrinos.

Figure 1 shows a realistic double-crossed spectrum that we will use as a reference case. We show antineutrinos as neutrinos with negative energy, and use n_ν to denote number densities. The dominant DLN is positive; the plasma is dominated by ν_e. There is a "flipped" range in both the ν and $\bar{\nu}$ sector, where the DLN is negative, i.e., opposite to the dominant one.

In this Letter, we show that $\bar{\nu}$ crossings emerge immediately after collapse, making slow instabilities the first to appear. Despite their name, they grow quickly enough to alter the flavor distribution well before angular crossings
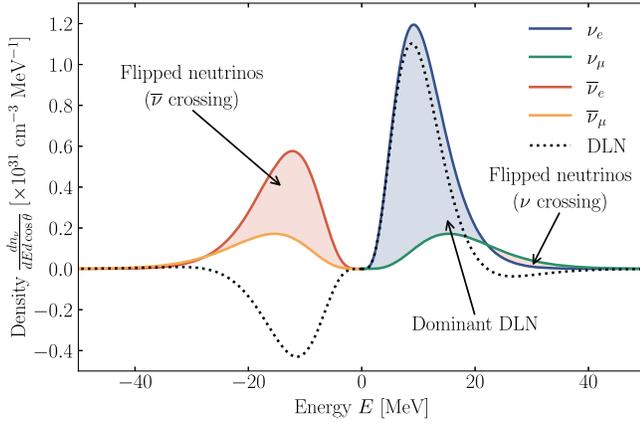
*Contact author: damianofg@gmail.com

FIG. 1. Double-crossed spectrum from our SN model at 62 ms post bounce, $r = 100$ km, and an angle to the radial direction of $\cos\theta = 0.6$ (asterisk in Fig. 2). Spectra reconstructed from discretized energy bins using a Gamma fit, as in Ref. [27]. The total (i.e., energy-integrated) DLN is positive; the positive contribution is highlighted with blue shade. A local excess in an energy interval of flipped neutrinos, with the opposite DLN (red shade), forms a spectral crossing and can cause an instability. Dotted line for DLN energy distribution.

develop, undermining any meaningful search for fast instabilities at later times, when the simulation has already become fundamentally inconsistent.

The mechanism by which these early slow instabilities arise is generic: after the neutronization burst, the $\bar\nu_e$ overshoot their heavy-flavor partners and cause a spectral crossing. We illustrate this development in a postprocessed SN simulation, exhibiting the progressive breakdown of the consistency of postprocessing, with stronger neutrino-mass-driven instabilities growing within tens of milliseconds. This early phase of SN evolution does not depend on detailed model assumptions or 3D effects, so our specific SN model is representative for the generic effect. We also stress that the wave numbers and growth rates of the slow instabilities follow from our recent analytic estimates [28]—they could not have been identified in a global numerical treatment.

Flavor instabilities—Flavor instabilities emerge in supernovae (SNe) when, relative to the dominant ν_e flux, a small population carries the "wrong"—opposite to the dominant one—lepton number. This role is played, in our two-flavor setup, by $\bar\nu_e$ or ν_μ. Flavor dynamics tries to avoid species that are wrong in this sense, so these subdominant species flip identity by emitting a flavomon—the quantum of the weak field they generate—through the decays $\bar\nu_e \to \bar\nu_\mu + \psi$ and $\nu_\mu \to \nu_e + \psi$. If there is an energy interval in which $\bar\nu_e$ dominate over $\bar\nu_\mu$, their decays dominate over the inverse reactions, causing an instability; the same can happen if there is an energy interval with ν_μ dominating over ν_e. The lepton number extracted from the flipped neutrinos is not lost, but converted to collective flavor waves and exchanged with the much larger ν_e flux. As more flavomons are

emitted, the field grows, representing CFC. A full account of this mechanism is provided in Supplemental Material (SM) [29].

Spectral $\bar\nu$ crossings are unavoidable in SN evolution, driven by the increasing $\bar\nu_e$ flux relative to $\bar\nu_\mu$ after core bounce. In addition, ν crossings may also occur, owing to the harder ν_μ spectra compared to ν_e. To assess whether "slow" CFCs can significantly affect the subsequent evolution, we must go beyond this qualitative picture and quantify when and where the crossings emerge, and how rapidly the resulting instabilities grow.

The answer requires solving the dispersion relation for collective modes, which arises from the quantum kinetic equation [67–71], linearized under the assumption of small flavomon field amplitude. The field evolves as a superposition of waves with wave vectors $\mathbf{K}$—assumed to satisfy $|\mathbf{K}| \gg \ell^{-1}$, where ℓ is the characteristic scale of SN inhomogeneities—each oscillating with frequency $\Omega_{\mathbf{K}}$ and possibly growing at a rate $\gamma_{\mathbf{K}}$.

Treating each $\mathbf{K}$ mode separately furnishes the dispersion relation in the form of an integral equation, which is surprisingly cumbersome to solve in practice. One needs to rely on root-finding algorithms in the manner of a black-box approach that obscures physical insight. We deliberately make the opposite choice and rely on the approximations developed in Refs. [7,13,28,72,73], which are derived from first principles and validated by comparison with SN-inspired numerical solutions. These formulas relate $\gamma_{\mathbf{K}}$ to the DLN parameters, providing a physical order-of-magnitude strategy.

Slow instabilities can display qualitatively distinct forms of behavior, depending on the underlying neutrino distribution. We identify three classes according to the depth of the spectral crossing, and elaborate in more detail in SM [29]. This subdivision is not redundant: the differences between these classes are the same as those between the bump-on-tail and beam-plasma instabilities in ordinary plasmas, emerging continuously from one another, yet with distinct physical properties [74].

For very shallow spectral crossings, we have *narrow slow instabilities* [28], due to the narrow resonance in the neutrino-flavomon interaction. These are *directional*, with flavomons emitted collinearly with the parent neutrinos.

The order of magnitude of $\gamma_{\mathbf{K}}$ is proportional to the energy splitting of neutrinos with opposite lepton number and energy E, which is $\omega_E = \delta m^2 \cos 2\vartheta / 2E$, with δm^2 the squared-mass splitting and ϑ the mixing angle in vacuum. For our estimates, we use the simple values $\delta m^2 = (50\ \mathrm{meV})^2$ and $\cos 2\vartheta = 1$. We employ natural units with $\hbar = c = 1$.

The DLN is dominated by ν_e, whereas the growth rate is proportional to the small fraction of flipped neutrinos carrying opposite lepton number. This result, derived in Ref. [28] and reviewed in SM [29], reveals that flavomons

moving in a direction $\cos\theta$ grow approximately with the rate

$$\gamma(\cos\theta) = \max_{|\mathbf{K}|}\gamma_{\mathbf{K}} \sim \frac{1}{\langle\omega_E^{-1}\rangle(\cos\theta)}\frac{dn_{\text{flip}}/d\cos\theta}{dn_{\text{DLN}}/d\cos\theta}. \quad (1)$$

Here n_{flip} is the number density of flipped neutrinos, those shaded in red in Fig. 1, whereas the average is taken over the DLN distribution in the form

$$\langle\omega_E^{-1}\rangle(\cos\theta) = \frac{\int_{-\infty}^{+\infty} dE \frac{dn_{\text{DLN}}}{dE d\cos\theta}\omega_E^{-1}}{\frac{dn_{\text{DLN}}}{d\cos\theta}}. \quad (2)$$

When the number of flipped neutrinos along a given direction reaches the total DLN along that direction, this estimate breaks down, transitioning into a *broad slow instability* [28,72]. The flavomon energy $\Omega_{\mathbf{K}}$ has a width $\gamma_{\mathbf{K}} \gg \omega_E$ and

$$\gamma(\cos\theta) = \max_{|\mathbf{K}|}\gamma_{\mathbf{K}} \sim \langle\omega_E\rangle(\cos\theta) \quad (3)$$

becomes the maximum growth rate in that direction—the neutrino beams can be approximated as monochromatic.

For very small DLN, the growth rate is enhanced by the small denominator $dn_{\text{DLN}}/d\cos\theta$ appearing in the average $\langle\omega_E\rangle(\cos\theta)$. The instability then enters a *nonresonant* regime, where it loses its directional character, i.e., neutrinos with any direction emit flavomons. This happens when γ becomes comparable with the refractive energy scale $\sqrt{2}G_F n_{\text{DLN}}$. (We previously identified this scale as $\mu\epsilon$, where $\mu = \sqrt{2}G_F n_\nu$ and $\epsilon = n_{\text{DLN}}/n_\nu$.) This regime, in which the growth rate scales as $\gamma \sim \sqrt{\omega_E\mu}$, never appears in SNe as it requires a very small DLN.

Our overall estimate of the slow-mode growth rates thus relies on Eqs. (1) and (3). Crucially, we associate a growth rate to each neutrino direction $\cos\theta$, which is physically interpreted as the growth rate of flavor waves moving in that particular direction.

Spectral crossings in SNe—To assess the impact of spectral crossings, we consider the fraction of flipped neutrinos, which actively emit flavomons. Angular crossings rely on a delicate balance of flavor-dependent angle distributions and depend sensitively on details and dimensionality of the simulations. In contrast, the dominance of $\bar\nu_e$ over $\bar\nu_\mu$ along certain directions is generic [75,76] due to the smaller, hotter decoupling region of $\bar\nu_\mu$. Additional effects, such as energy degradation via nucleon scattering and positive temperature gradients in accreting models, reinforce this feature. Hence, the details of the SN model do not significantly affect our results.

We use a numerical model with available angle and energy distributions [77], namely a spherically symmetric SN simulation of the Garching group, computed with PROMETHEUS-VERTEX. This code includes energy-dependent three-species neutrino transport with relativistic corrections and state-of-the-art microphysics. The progenitor is a

$13.8M_\odot$ model of Refs. [78,79], the EOS the one of Lattimer and Swesty with incompressibility of 180 MeV [80], though results with 220 MeV are nearly identical during the first 100 ms postbounce. The model does not explode, which is irrelevant at a few tens of milliseconds. Details of the model are found in Ref. [81].

Spherical symmetry is also not a limiting assumption, as 3D effects are small when slow instabilities develop at some 10 ms after bounce. Their properties are governed by generic outflow features—notably the growing dominance of $\bar\nu_e$ over $\bar\nu_\mu$ caused by the shock-heated PNS mantle rapidly growing by high postbounce mass accretion rates—justifying the use of a single representative model.

We first test whether a spectral crossing exists at all, of both the $\bar\nu$ and ν type. For each time, radius, and neutrino direction, we determine the total number of flipped $\bar\nu$ (number of $\bar\nu_e$ in excess of $\bar\nu_x$ in every energy bin) and ν (same for ν_μ in excess of ν_e). The concrete definition, e.g., for $\bar\nu$, is the ratio between the red-shaded area for negative energies in Fig. 1 and the energy-integrated DLN. In Fig. 2, we highlight with a red (blue) contour the regions containing a spectral crossing.

Crossings of $\bar\nu$ appear immediately and over extended regions. They arise first because, while the $\bar\nu_e$ and $\bar\nu_\mu$ fluxes are comparable, the $\bar\nu_\mu$ are more forward directed, causing a $\bar\nu_e$ excess in nonforward directions already within the $\bar\nu_e$ sphere. With time, the overall $\bar\nu_e$ flux dominates over $\bar\nu_\mu$ and the crossing extends even to forward directions. Meanwhile, a ν crossing, corresponding to a high-energy excess of ν_μ over ν_e, becomes progressively more significant in the forward direction. However, it is less prominent and occurs after $\bar\nu$ crossings, which thus could affect the appearance of ν crossings.

Since $\bar\nu$ crossings dominate, we show the fraction of flipped $\bar\nu_e$ in Fig. 2 by color coding, providing a direct handle on the importance of CFCs triggered by spectral crossings; this is defined as the integral of the red-shaded area for negative energies in Fig. 1 divided by the energy-integrated number of $\bar\nu_e$. Already at early times, up to 40% of antineutrinos along nonforward directions are flipped and will emit flavomons, and this fraction strongly increases with time, even reaching up to 100%. These spectral crossings develop well below the shock wave, suggesting a potential impact on the explosion.

Dynamical impact—Spectral crossings alone are not enough to assure a dynamical impact. We need to demonstrate that the resulting instabilities are rapid enough to (i) outpace the rate of beta interactions, which compete with the decay $\bar\nu_e \to \bar\nu_\mu + \psi$ in pinning neutrinos to their flavor states, and (ii) grow substantially to become nonlinear over the dynamical timescale $t_{\text{dyn}} \sim r$ for neutrino propagation through the SN. This estimate for t_{dyn} is only approximate because flavomons propagate through a radial profile with a space-changing growth rate. For an order-of-magnitude estimate, we may still assume that there is a single relevant
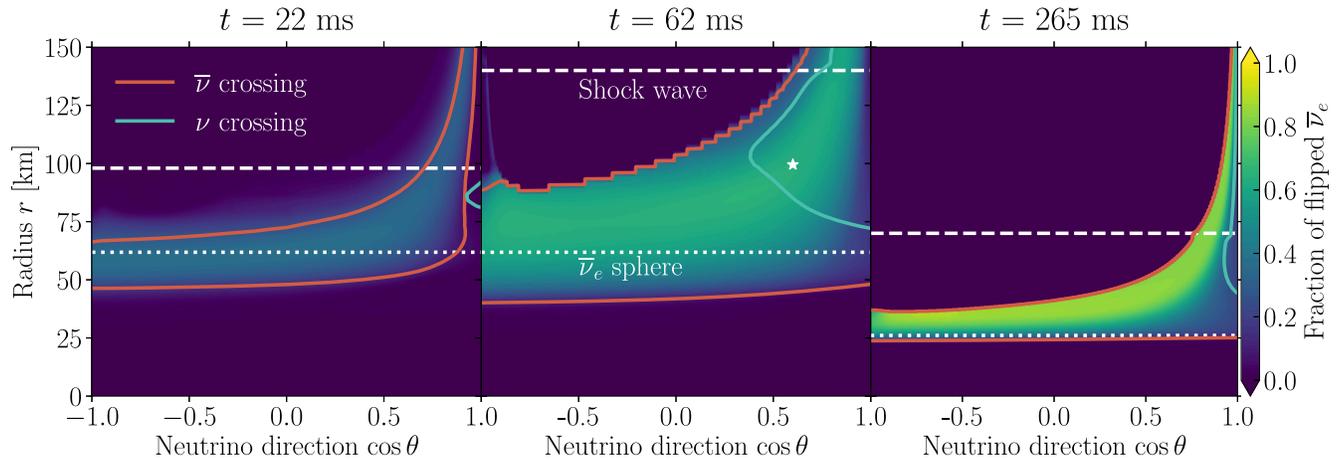
FIG. 2. Fraction of flipped $\bar{\nu}_e$ color coded as a function of radius and direction at different times. Regions exhibiting a $\bar{\nu}$ or ν crossing are indicated by colored lines, using a threshold of 5% for the flipped fraction. We show the shock wave radius (dashed white line) and the $\bar{\nu}_e$ sphere (dotted white lien), defined as the radius where the $\bar{\nu}_e$ number flux equals one-quarter of the density. The number-changing reactions for $\bar{\nu}_\mu$ freeze out much deeper inside. The asterisk marks the location for the energy distribution shown in Fig. 1.

length scale, namely the radius itself. A full study of the propagation through a stratified environment is beyond our scope; more comments are provided in SM [29].

We estimate the growth rate from the smallest among Eqs. (1) and (3), determining which class is relevant. To assess the dynamical impact, we use the number of e-folds γr developed over the dynamical timescale. When it strongly exceeds unity, the instability develops fully. To estimate the role of collisions, we compare the growth rate with the energy-averaged $\nu_e n \rightarrow e^- p$ rate, taken from from Eq. (11) of Ref. [82].

Figure 3 shows the γr (e-folds) distribution. Initially nonforward directions dominate the instability, as the forward-peaked $\bar{\nu}_x$ suppress spectral crossings. Later, $\bar{\nu}_e$ dominate across the entire angular range. As time progresses, the instability strengthens with the increasing population of flipped neutrinos, eventually entering the broad regime, within the region marked by the blue line. However, the growth rate remains below that of fast instabilities and never reaches the nonresonant limit $\gamma \sim \sqrt{\omega_E \mu}$, confirming the findings of Refs. [28,72,73]. Except for a narrow region below 50 km, the growth rate exceeds that of beta reactions, so collisions do not hinder the instability. This illustrates the central point of our Letter: within tens of milliseconds, slow instabilities grow rapidly enough to alter the flavor distribution.

Discussion—Spectral crossings are generic in SNe. We have shown that $\bar{\nu}$ crossings, caused by $\bar{\nu}_e$ dominating over $\bar{\nu}_\mu$, induce instabilities rapid enough to alter flavor evolution within tens of milliseconds after bounce. The affected region starts below the $\bar{\nu}_e$ sphere and reaches beyond the shock wave. The impact on shock revival is difficult to assess without understanding the nonlinear feedback on the medium. At early times, the instability is driven by flipped $\bar{\nu}_e$, so CFCs will attempt to remove them via $\bar{\nu}_e \rightarrow \bar{\nu}_\mu + \psi$,

suggesting negative feedback on the explosion by reducing the rate of energy deposition. Later effects such as ν crossings, which would tend in the opposite direction by converting high-energy $\nu_\mu \rightarrow \nu_e + \psi$, cannot be captured consistently by postprocessing. Most importantly, at the early times of interest here, no angular crossing develops [26], so there are no fast instabilities.

While we use a specific numerical SN model for convenience, our argument for the early emergence of slow instabilities is generic. $\bar{\nu}$ crossings always lead to instability [83], and they only require a directional dominance of $\bar{\nu}_e$ over $\bar{\nu}_\mu$. In the core, such crossing is precluded by chemical equilibrium, with $\bar{\nu}_e$ suppressed by a negative chemical potential, but outside of the core $\bar{\nu}$ crossings are induced by the luminosity of accretion-powered $\bar{\nu}_e$ overtaking $\bar{\nu}_\mu$ (see, e.g., Fig. 2 of Ref. [84]).

These slow instabilities are quite insidious: their wavelengths are even millimeters at these early times, they oscillate over picoseconds, yet grow only over tens of microseconds [28,72,73]. This is quick enough to alter flavor evolution in SNe, yet slow compared with their rapid oscillations as to obstruct numerical analysis. Conversely, they grow so slowly that their initial amplitude is another concern, a question deferred to SM [29]. Even worse, their initial growth timescale is comparable with the dynamical timescale of escaping neutrinos, so their evolution is nonlocal. Flavomons themselves have a preferred direction along the streaming velocity, initially slightly nonforward, and later entirely in the forward direction. A possible way forward is to treat flavomons as independent degrees of freedom, with their own streaming velocity, affected by the inhomogeneity of the medium [30,73,85].

It is well known, of course, that neutrino-mass-driven instabilities may appear without angular crossings. Reference [86] noted that close to an angular crossing,
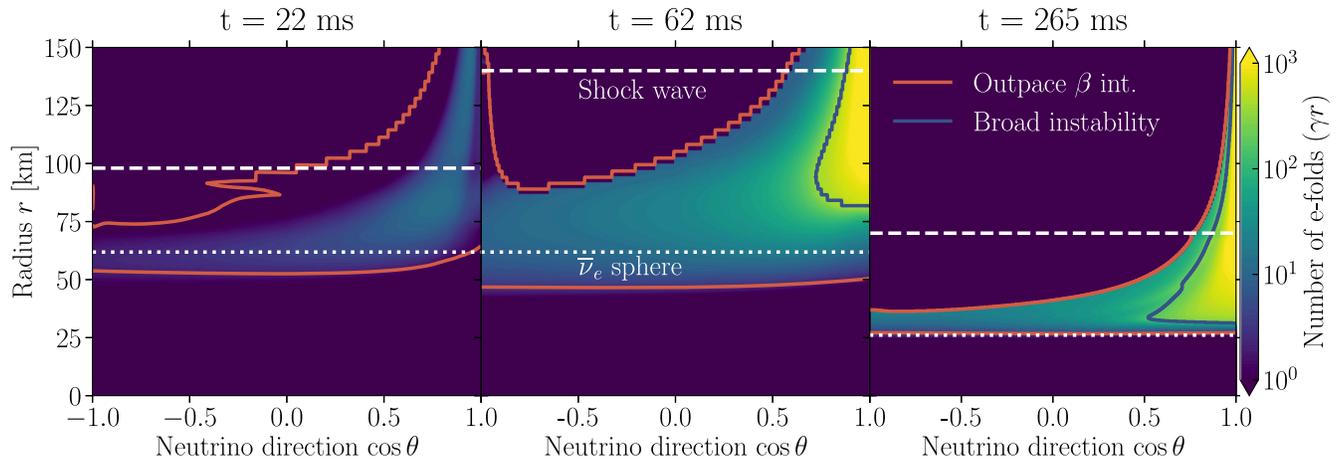
FIG. 3. Number of e-folds induced by the growth of slow instabilities as a function of neutrino location and direction. The panel layout and the positions of neutrinospheres and shock waves are the same as in Fig. 2.

slow instabilities might appear—their reference cases show broad or nonresonant ones—and Ref. [87] has identified such conditions at about 50 ms. Our configurations, however, are far from an angular crossing and mainly produce narrow slow instabilities. With millimeter to centimeter scales, one can find them only with our analytic tools. Beyond identifying these early slow instabilities, we highlight their implications: the induced flavor conversions jeopardize the later appearance of angular crossings, or at least any robust conclusions about their existence.

In the innermost region (below 50 km), spectral crossings occur where beta reactions are fast. Collisions may here suppress the instability or trigger a collisional instability (CFI) [88]. However, this requires not only a spectral crossing, but also a sufficiently large ν_e–$\bar{\nu}_e$ asymmetry. An approximate condition is $n_{\nu_e}/\Gamma_{\nu_e} \lesssim n_{\bar{\nu}_e}/\Gamma_{\bar{\nu}_e}$, where Γ_ν is the beta reaction rate [28]. Since $\Gamma_{\nu_e}/\Gamma_{\bar{\nu}_e} \sim n_n/n_p$, this implies $n_{\bar{\nu}_e} \gtrsim n_{\nu_e} n_p/n_n$, with n_n and n_p the neutron and proton densities and Pauli blocking was neglected. This condition is only marginally satisfied in our simulation, mostly in regions where the slow instability growth rate is much larger than the beta rate.

Hence, since CFI have a threshold, unlike slow instabilities, they are generically less important. This conclusion is strongly vindicated by a recent study [89], showing that the typical growth rate of CFIs is $\gamma \sim 100$ s^{-1}, generally smaller than the ones of slow instabilities in our Letter, which start at $\gamma \sim 10^{-1}$ km$^{-1} \sim 10^4$ s^{-1} at 20 ms, but rapidly grow larger by several orders of magnitude as the crossing gets deeper. At a few 100 ms, CFIs appear in the PNS convective region with larger growth rates due to the small ν_e–$\bar{\nu}_e$ asymmetry, which however is long after the first appearance of slow instabilities.

We finally stress again that searching for instabilities by postprocessing numerical simulations is a purely diagnostic tool. At best, the only realistic instabilities are the first ones to appear. Figure 3 illustrates the progressive breakdown of postprocessing. At early times, instabilities are found in a narrow region with small growth rate, whereas later, the number of e-folds becomes progressively larger, signaling a complete loss of realism. This picture agrees with the message highlighted in Refs. [7,13,28,72,73,85] that weak instabilities are the only ones that can be consistently inferred from postprocessing. Already at about 20 ms, CFCs will prevent the emergence of strong instabilities. Moreover, since these slow instabilities appear already at tens of milliseconds, long before angular crossings [26], the impact of the latter is directly questioned.

A similar reexamination of what are the first and therefore most important instabilities is also needed for neutron-star mergers, where postprocessing reveals ubiquitous fast instabilities (see, e.g., Refs. [90–93]). We plan to address this question in the future.

Data availability—The data that support the findings of this article are openly available [81].

[1] S. A. Colgate and R. H. White, The hydrodynamic behavior of supernovae explosions, Astrophys. J. **143**, 626 (1966).

[2] H. A. Bethe and J. R. Wilson, Revival of a stalled supernova shock by neutrino heating, Astrophys. J. **295**, 14 (1985).

[3] H.-T. Janka, Explosion mechanisms of core-collapse supernovae, Annu. Rev. Nucl. Part. Sci. **62**, 407 (2012).

[4] I. Tamborra and S. Shalgar, New developments in flavor evolution of a dense neutrino gas, Annu. Rev. Nucl. Part. Sci. **71**, 165 (2021).

[5] M. C. Volpe, Neutrinos from dense environments: Flavor mechanisms, theoretical approaches, observations, and new directions, Rev. Mod. Phys. **96**, 025004 (2024).

[6] L. Johns, S. Richers, and M.-R. Wu, Neutrino oscillations in core-collapse supernovae and neutron star mergers, Annu. Rev. Nucl. Part. Sci. **75** (2025).

[7] D. F. G. Fiorillo and G. G. Raffelt, Theory of neutrino fast flavor evolution. Part I. Linear response theory and stability conditions., J. High Energy Phys. 08 (2024) 225.

[8] H. Nagakura, Roles of fast neutrino-flavor conversion on the neutrino-heating mechanism of core-collapse supernova, Phys. Rev. Lett. **130**, 211401 (2023).

[9] J. Ehring, S. Abbar, H.-T. Janka, G. Raffelt, and I. Tamborra, Fast neutrino flavor conversion in core-collapse supernovae: A parametric study in 1D models, Phys. Rev. D **107**, 103034 (2023).

[10] J. Ehring, S. Abbar, H.-T. Janka, G. Raffelt, and I. Tamborra, Fast neutrino flavor conversions can help and hinder neutrino-driven explosions, Phys. Rev. Lett. **131**, 061401 (2023).

[11] T. Wang and A. Burrows, The effect of the fast-flavor instability on core-collapse supernova models, Astrophys. J. **986**, 153 (2025).

[12] L. Johns, Subgrid modeling of neutrino oscillations in astrophysics, Phys. Rev. D **112**, 043024 (2025).

[13] D. F. G. Fiorillo and G. G. Raffelt, Theory of neutrino fast flavor evolution. Part II. Solutions at the edge of instability, J. High Energy Phys. 12 (2024) 205.

[14] I. Izaguirre, G. Raffelt, and I. Tamborra, Fast pairwise conversion of supernova neutrinos: A dispersion-relation approach, Phys. Rev. Lett. **118**, 021101 (2017).

[15] I. Tamborra, L. Hüdepohl, G. Raffelt, and H.-T. Janka, Flavor-dependent neutrino angular distribution in core-collapse supernovae, Astrophys. J. **839**, 132 (2017).

[16] S. Shalgar and I. Tamborra, On the occurrence of crossings between the angular distributions of electron neutrinos and antineutrinos in the supernova core, Astrophys. J. **883**, 80 (2019).

[17] T. Morinaga, H. Nagakura, C. Kato, and S. Yamada, Fast neutrino-flavor conversion in the preshock region of core-collapse supernovae, Phys. Rev. Res. **2**, 012046 (2020).

[18] F. Capozzi, S. Abbar, R. Bollig, and H.-T. Janka, Fast neutrino flavor conversions in one-dimensional core-collapse supernova models with and without muon creation, Phys. Rev. D **103**, 063013 (2021).

[19] M. Cornelius, I. Tamborra, M. Heinlein, S. Shalgar, and H.-T. Janka, Electron-neutrino lepton number crossings: Variations with the supernova core physics, Phys. Rev. D **112**, 063006 (2025).

[20] S. Abbar, H. Duan, K. Sumiyoshi, T. Takiwaki, and M. C. Volpe, On the occurrence of fast neutrino flavor conversions in multidimensional supernova models, Phys. Rev. D **100**, 043004 (2019).

[21] H. Nagakura, T. Morinaga, C. Kato, and S. Yamada, Fast-pairwise collective neutrino oscillations associated with asymmetric neutrino emissions in core-collapse supernovae, Astrophys. J. **886**, 139 (2019).

[22] M. Delfan Azari, S. Yamada, T. Morinaga, H. Nagakura, S. Furusawa, A. Harada, H. Okawa, W. Iwakami, and K. Sumiyoshi, Fast collective neutrino oscillations inside the neutrino sphere in core-collapse supernovae, Phys. Rev. D **101**, 023018 (2020).

[23] S. Abbar, H. Duan, K. Sumiyoshi, T. Takiwaki, and M. C. Volpe, Fast neutrino flavor conversion modes in multidimensional core-collapse supernova models: The role of the asymmetric neutrino distributions, Phys. Rev. D **101**, 043016 (2020).

[24] R. Glas, H.-T. Janka, F. Capozzi, M. Sen, B. Dasgupta, A. Mirizzi, and G. Sigl, Fast neutrino flavor instability in the neutron-star convection layer of three-dimensional supernova models, Phys. Rev. D **101**, 063001 (2020).

[25] S. Abbar, F. Capozzi, R. Glas, H.-T. Janka, and I. Tamborra, On the characteristics of fast neutrino flavor instabilities in three-dimensional core-collapse supernova models, Phys. Rev. D **103**, 063033 (2021).

[26] H. Nagakura, L. Johns, A. Burrows, and G. M. Fuller, Where, when, and why: Occurrence of fast-pairwise collective neutrino oscillation in three-dimensional core-collapse supernova models, Phys. Rev. D **104**, 083025 (2021).

[27] I. Tamborra, B. Müller, L. Hüdepohl, H.-T. Janka, and G. Raffelt, High-resolution supernova neutrino spectra represented by a simple fit, Phys. Rev. D **86**, 125031 (2012).

[28] D. F. G. Fiorillo and G. G. Raffelt, Dispersion relation of the neutrino plasma: Unifying fast, slow, and collisional instabilities, arXiv:2505.20389.

[29] See Supplemental Material at http://link.aps.org/supplemental/10.1103/jbmx-rbzt for a review of the theory of flavor kinetic instabilities, meant as a guide to both the results and to the pertinent literature. We also report the properties of the slow instabilities in our SN model for more time snapshots than shown in the main text, which includes Refs. [30–66].

[30] D. F. G. Fiorillo and G. G. Raffelt, Fast flavor conversions at the edge of instability in a two-beam model, Phys. Rev. Lett. **133**, 221004 (2024).

[31] D. F. G. Fiorillo and G. G. Raffelt, Slow and fast collective neutrino oscillations: Invariants and reciprocity, Phys. Rev. D **107**, 043024 (2023).

[32] D. F. G. Fiorillo and G. G. Raffelt, Flavor solitons in dense neutrino gases, Phys. Rev. D **107**, 123024 (2023).

[33] D. F. G. Fiorillo, M. Goimil-García, and G. G. Raffelt, Fast flavor pendulum: Instability condition, Phys. Rev. D **111**, 083028 (2025).

[34] L. Johns, Implications of conservation laws and ergodicity for neutrino flavor instability, Phys. Rev. D **112**, 063029 (2025).

[35] T. Morinaga, Fast neutrino flavor instability and neutrino flavor lepton number crossings, Phys. Rev. D **105**, L101301 (2022).

[36] B. Dasgupta, Collective neutrino flavor instability requires a crossing, Phys. Rev. Lett. **128**, 081102 (2022).

[37] S. Samuel, Neutrino oscillations in dense neutrino gases, Phys. Rev. D **48**, 1462 (1993).

[38] S. Hannestad, G. G. Raffelt, G. Sigl, and Y. Y. Y. Wong, Self-induced conversion in dense neutrino gases: Pendulum in flavor space, Phys. Rev. D **74**, 105010 (2006); **76**, 029901 (E) (2007).

[39] D. F. G. Fiorillo, I. Padilla-Gay, and G. G. Raffelt, Collisions and collective flavor conversion: Integrating out the fast dynamics, Phys. Rev. D **109**, 063021 (2024).

[40] F. Capozzi, B. Dasgupta, E. Lisi, A. Marrone, and A. Mirizzi, Fast flavor conversions of supernova neutrinos: Classifying instabilities via dispersion relations, Phys. Rev. D **96**, 043016 (2017).

[41] C. Yi, L. Ma, J. D. Martin, and H. Duan, Dispersion relation of the fast neutrino oscillation wave, Phys. Rev. D **99**, 063005 (2019).

[42] L. Johns and A. Kost, Local-equilibrium theory of neutrino oscillations, arXiv:2506.03271.

[43] S. Bhattacharyya, M.-R. Wu, and Z. Xiong, Role of matter inhomogeneity on fast flavor conversion of supernova neutrinos, arXiv:2504.11316.

[44] I. Padilla-Gay, I. Tamborra, and G. G. Raffelt, Neutrino flavor pendulum reloaded: The case of fast pairwise conversion, Phys. Rev. Lett. **128**, 121102 (2022).

[45] L. Johns, H. Nagakura, G. M. Fuller, and A. Burrows, Neutrino oscillations in supernovae: Angular moments and fast instabilities, Phys. Rev. D **101**, 043009 (2020).

[46] G. G. Raffelt, N-mode coherence in collective neutrino oscillations, Phys. Rev. D **83**, 105022 (2011); **104**, 089902(E) (2021).

[47] Y. Pehlivan, A. B. Balantekin, T. Kajino, and T. Yoshida, Invariants of collective neutrino oscillations, Phys. Rev. D **84**, 065008 (2011).

[48] S. Bhattacharyya and B. Dasgupta, Fast flavor depolarization of supernova neutrinos, Phys. Rev. Lett. **126**, 061302 (2021).

[49] H. Nagakura and M. Zaizen, Time-dependent and quasisteady features of fast neutrino-flavor conversion, Phys. Rev. Lett. **129**, 261101 (2022).

[50] M. Zaizen and H. Nagakura, Simple method for determining asymptotic states of fast neutrino-flavor conversion, Phys. Rev. D **107**, 103022 (2023).

[51] M. Zaizen and H. Nagakura, Characterizing quasisteady states of fast neutrino-flavor conversion by stability and conservation laws, Phys. Rev. D **107**, 123021 (2023).

[52] Z. Xiong, M.-R. Wu, S. Abbar, S. Bhattacharyya, M. George, and C.-Y. Lin, Evaluating approximate asymptotic distributions for fast neutrino flavor conversions in a periodic 1D box, Phys. Rev. D **108**, 063003 (2023).

[53] M. Cornelius, S. Shalgar, and I. Tamborra, Perturbing fast neutrino flavor conversion, J. Cosmol. Astropart. Phys. 02 (2024) 038.

[54] Z. Xiong, M.-R. Wu, M. George, and C.-Y. Lin, Robust integration of fast flavor conversions in classical neutrino transport, Phys. Rev. Lett. **134**, 051003 (2025).

[55] S. Abbar, M.-R. Wu, and Z. Xiong, Application of neural networks for the reconstruction of supernova neutrino energy spectra following fast neutrino flavor conversions, Phys. Rev. D **109**, 083019 (2024).

[56] I. Padilla-Gay, H.-H. Chen, S. Abbar, M.-R. Wu, and Z. Xiong, Flavor equilibration of supernova neutrinos: Exploring the dynamics of slow modes, Phys. Rev. D **112**, 043039 (2025).

[57] A. A. Vedenov, E. P. Velikhov, and R. Z. Sagdeev, Quasilinear theory of plasma oscillations, Technical Report, Kurchatov Institute of Atomic Energy, Moscow, 1962, https://www.osti.gov/biblio/4726983.

[58] W. E. Drummond and D. Pines, Non-linear stability of plasma oscillation, Technical Report, General Atomic Division, General Dynamics Corp., San Diego, CA, 1961, https://www-thphys.physics.ox.ac.uk/people/Alexander Schekochihin/notes/PlasmaClassics/drummond_pines62.pdf.

[59] W. E. Drummond and D. Pines, Non-linear plasma oscillation, Ann. Phys. (N.Y.) **28**, 478 (1964).

[60] A. A. Schekochihin, Lectures on kinetic theory and magnetohydrodynamics of plasmas. Lecture notes for the Oxford MMathPhys/MScMTP programme (2024), https://www-thphys.physics.ox.ac.uk/people/mbarnes/teaching/stat_phys/A1LectureNotes_AAS_MT17.pdf.

[61] J. F. Cherry, J. Carlson, A. Friedland, G. M. Fuller, and A. Vlasenko, Neutrino scattering and flavor transformation in supernovae, Phys. Rev. Lett. **108**, 261104 (2012).

[62] S. Sarikas, I. Tamborra, G. Raffelt, L. Hudepohl, and H.-T. Janka, Supernova neutrino halo and the suppression of self-induced flavor conversion, Phys. Rev. D **85**, 113007 (2012).

[63] J. F. Cherry, J. Carlson, A. Friedland, G. M. Fuller, and A. Vlasenko, Halo modification of a supernova neutronization neutrino burst, Phys. Rev. D **87**, 085037 (2013).

[64] V. Cirigliano, M. Paris, and S. Shalgar, Collective neutrino oscillations with the halo effect in single-angle approximation, J. Cosmol. Astropart. Phys. 11 (2018) 019.

[65] M. Zaizen, J. F. Cherry, T. Takiwaki, S. Horiuchi, K. Kotake, H. Umeda, and T. Yoshida, Neutrino halo effect on collective neutrino oscillation in iron core-collapse supernova model of a $9.6M_\odot$ star, J. Cosmol. Astropart. Phys. 06 (2020) 011.

[66] S. Abbar and F. Capozzi, Suppression of fast neutrino flavor conversions occurring at large distances in core-collapse supernovae, J. Cosmol. Astropart. Phys. 03 (2022) 051.

[67] A. D. Dolgov, Neutrinos in the early Universe, Yad. Fiz. **33**, 1309 (1981) [Sov. J. Nucl. Phys. **33**, 700 (1981)].

[68] M. A. Rudzsky, Kinetic equations for neutrino spin- and type-oscillations in a medium, Astrophys. Space Sci. **165**, 65 (1990).

[69] G. Sigl and G. Raffelt, General kinetic description of relativistic mixed neutrinos, Nucl. Phys. **B406**, 423 (1993).

[70] D. F. G. Fiorillo, G. G. Raffelt, and G. Sigl, Inhomogeneous kinetic equation for mixed neutrinos: Tracing the missing energy, Phys. Rev. Lett. **133**, 021002 (2024).

[71] D. F. G. Fiorillo, G. G. Raffelt, and G. Sigl, Collective neutrino-antineutrino oscillations in dense neutrino environments?, Phys. Rev. D **109**, 043031 (2024).

[72] D. F. G. Fiorillo and G. G. Raffelt, Theory of neutrino slow flavor evolution. Part I. Homogeneous medium, J. High Energy Phys. 04 (2025) 146.

[73] D. F. G. Fiorillo and G. G. Raffelt, Theory of neutrino slow flavor evolution. Part II. Space-time evolution of linear instabilities, J. High Energy Phys. 06 (2025) 146.

[74] T. J. M. Boyd and J. J. Sanderson, *The Physics of Plasmas* (Cambridge University Press, Cambridge, England, 2003).

[75] H.-T. Janka, When do supernova neutrinos of different flavors have similar luminosities but different spectra?, Astropart. Phys. **3**, 377 (1995).

[76] G. G. Raffelt, Muon-neutrino and tau-neutrino spectra formation in supernovae, Astrophys. J. **561**, 890 (2001).

[77] P. D. Serpico, S. Chakraborty, T. Fischer, L. Hüdepohl, H.-T. Janka, and A. Mirizzi, Probing the neutrino mass hierarchy with the rise time of a supernova burst, Phys. Rev. D **85**, 085031 (2012).

[78] S. E. Woosley, A. Heger, and T. A. Weaver, The evolution and explosion of massive stars, Rev. Mod. Phys. **74**, 1015 (2002).

[79] S. E. Woosley and T. A. Weaver, The evolution and explosion of massive stars. 2. Explosive hydrodynamics and nucleosynthesis, Astrophys. J. Suppl. Ser. **101**, 181 (1995).

[80] J. M. Lattimer and D. F. Swesty, A generalized equation of state for hot, dense matter, Nucl. Phys. **A535**, 331 (1991).

[81] The Garching core-collapse supernova research archive, https://wwwmpa.mpa-garching.mpg.de/ccsnarchive/.

[82] H.-T. Janka, Conditions for shock revival by neutrino heating in core collapse supernovae, Astron. Astrophys. **368**, 527 (2001).

[83] D. F. G. Fiorillo and G. G. Raffelt, Lepton number crossings are insufficient for flavor instabilities, arXiv:2507.22987.

[84] D. F. G. Fiorillo, M. Heinlein, H.-T. Janka, G. Raffelt, E. Vitagliano, and R. Bollig, Supernova simulations confront SN 1987A neutrinos, Phys. Rev. D **108**, 083040 (2023).

[85] D. F. G. Fiorillo and G. G. Raffelt, Collective flavor conversions are interactions of neutrinos with quantized flavor waves, Phys. Rev. Lett. **134**, 211003 (2025).

[86] P. Dedin Neto, I. Tamborra, and S. Shalgar, Energy dependence of flavor instabilities stemming from crossings in the neutrino flavor lepton number angular distribution, arXiv:2312.06556.

[87] S. Shalgar and I. Tamborra, Neutrino quantum kinetics in a core-collapse supernova, J. Cosmol. Astropart. Phys. 09 (2024) 021.

[88] L. Johns, Collisional flavor instabilities of supernova neutrinos, Phys. Rev. Lett. **130**, 191001 (2023).

[89] T. Wang, H. Nagakura, L. Johns, and A. Burrows, Effect of the collisional flavor instability on core-collapse supernova models, Phys. Rev. D **112**, 063039 (2025).

[90] M.-R. Wu and I. Tamborra, Fast neutrino conversions: Ubiquitous in compact binary merger remnants, Phys. Rev. D **95**, 103007 (2017).

[91] M.-R. Wu, I. Tamborra, O. Just, and H.-T. Janka, Imprints of neutrino-pair flavor conversions on nucleosynthesis in ejecta from neutron-star merger remnants, Phys. Rev. D **96**, 123015 (2017).

[92] X. Li and D. M. Siegel, Neutrino fast flavor conversions in neutron-star postmerger accretion disks, Phys. Rev. Lett. **126**, 251101 (2021).

[93] H. Nagakura, K. Sumiyoshi, S. Fujibayashi, Y. Sekiguchi, and M. Shibata, Neutrino flavor instabilities in a binary neutron star merger remnant: Roles of a long-lived hypermassive neutron star, Phys. Rev. D **112**, 043029 (2025).